

Applied Mathematics Research Program Annual PI Meeting
May 22 - 24, 2007, LLNL

Models and Computational Algorithms for Multiphase Magnetohydrodynamics

Roman Samulyak

*Computational Science Center
Brookhaven National Laboratory*

Collaborators: MHD Algorithms and Applications:

Tianshi Lu, *CSC/BNL, modeling, software development, fusion applications*

Jian Du, *Stony Brook University, software development, accelerator applications*

Paul Parks, *General Atomics, MHD theory, fusion applications*

Front Tracking and Multiphase Flows:

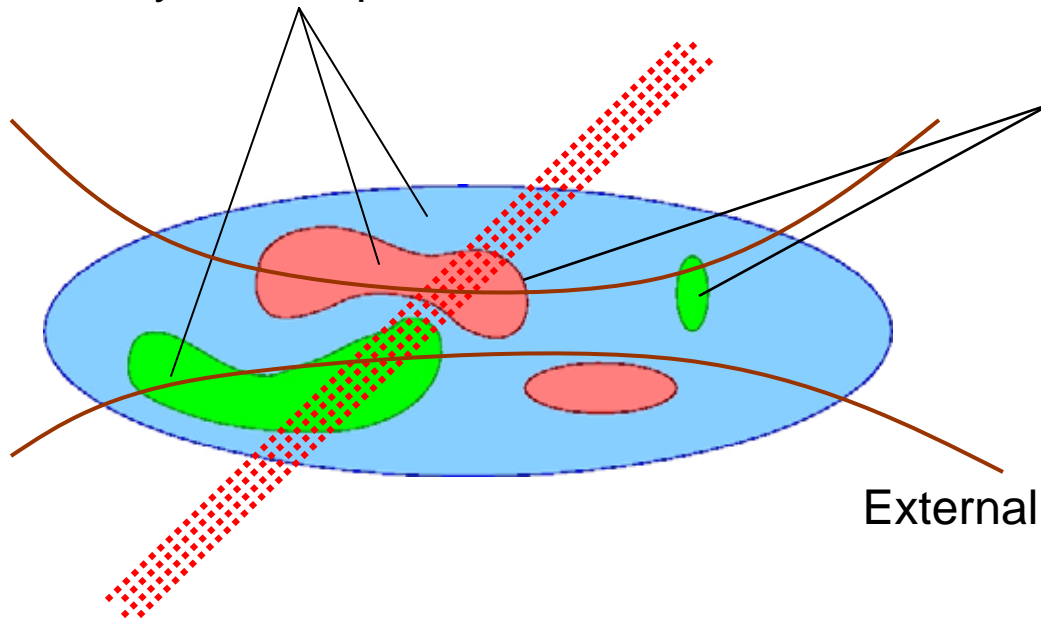
James Glimm, *Stony Brook University / BNL*

Xiaolin Li, *Stony Brook University*

Multiphase MHD: Schematic

Phases:

- Compressible fluid or gas
- Conducting liquids or weakly ionized plasma
- Fully ionized plasma



Material interfaces:

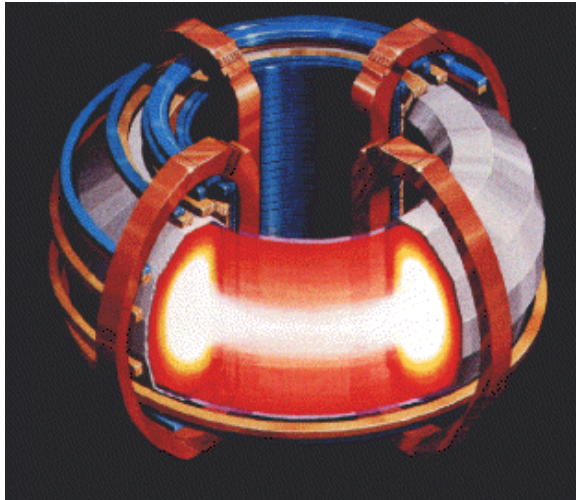
- Discontinuity of density and physics properties (electrical conductivity)
- Governed by the Riemann problem for MHD equations or phase transition equations

External magnetic field

External sources:

- Intense particle beams
- Laser pulses

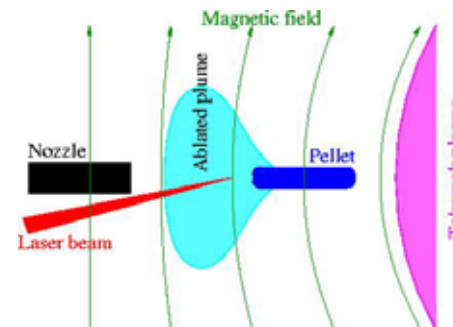
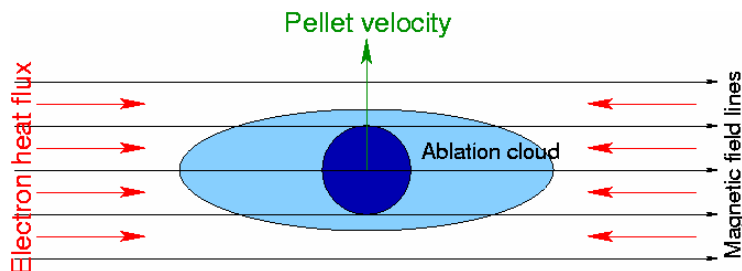
Motivation



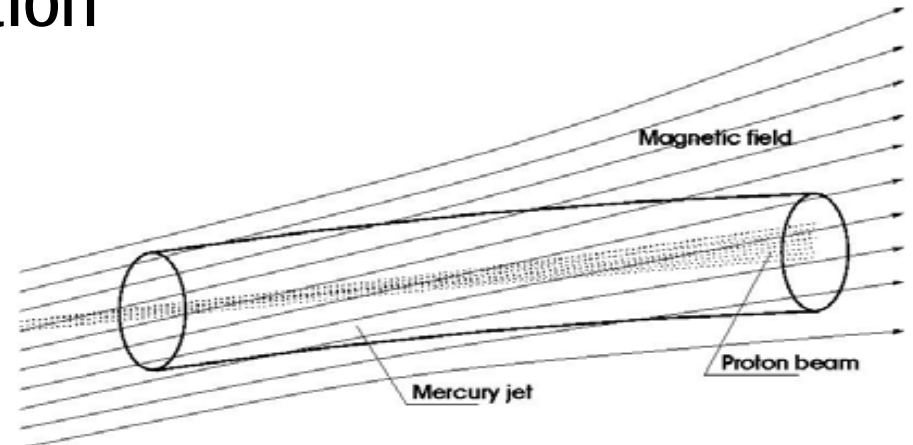
Tokamak applications

- Pellet fueling of tokamaks
- Striation instabilities
- Laser driven pellet acceleration
- Gyrotron driven pellet acceleration
- “Killer-pellets” for plasma disruption mitigation
- Liquid jet for plasma disruption mitigation

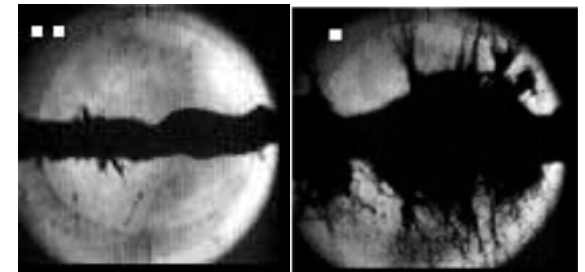
Schematic of the pellet ablation



Laser driven pellet acceleration



Neutrino Factory / Muon Collider target has been proposed as a free mercury jet interacting with an intensive proton pulse in a 20Tesla magnetic field



Models and Numerical Algorithms (talk outline)

- Numerical algorithms for coupled the hyperbolic - elliptic system in domains with moving, geometrically complex boundaries
 - Front tracking method for material interfaces
- Phase transition models (vaporization and ablation)
- Validation of the MHD code
- Simulation of accelerator targets and pellet fueling of tokamaks

MHD equations and approximations

Full system of MHD equations

$$\frac{\partial \rho}{\partial t} = -\nabla \cdot (\rho \mathbf{u})$$

$$\rho \left(\frac{\partial}{\partial t} + \mathbf{u} \cdot \nabla \right) \mathbf{u} = -\nabla P + \mu \Delta \mathbf{u} + \frac{1}{c} (\mathbf{J} \times \mathbf{B})$$

$$\rho \left(\frac{\partial}{\partial t} + \mathbf{u} \cdot \nabla \right) e = -P \nabla \cdot \mathbf{u} + \frac{1}{\sigma} \mathbf{J}^2$$

$$\frac{\partial \mathbf{B}}{\partial t} = \nabla \times (\mathbf{u} \times \mathbf{B}) - \nabla \times \left(\frac{c^2}{4\pi\sigma} \nabla \times \mathbf{B} \right)$$

$$P = P(\rho, e), \quad \nabla \cdot \mathbf{B} = 0$$

Low magnetic Re approximation

$$\text{Re}^M = \frac{uL\sigma}{c^2} \ll 1, \quad \frac{\delta B}{B} \ll 1$$

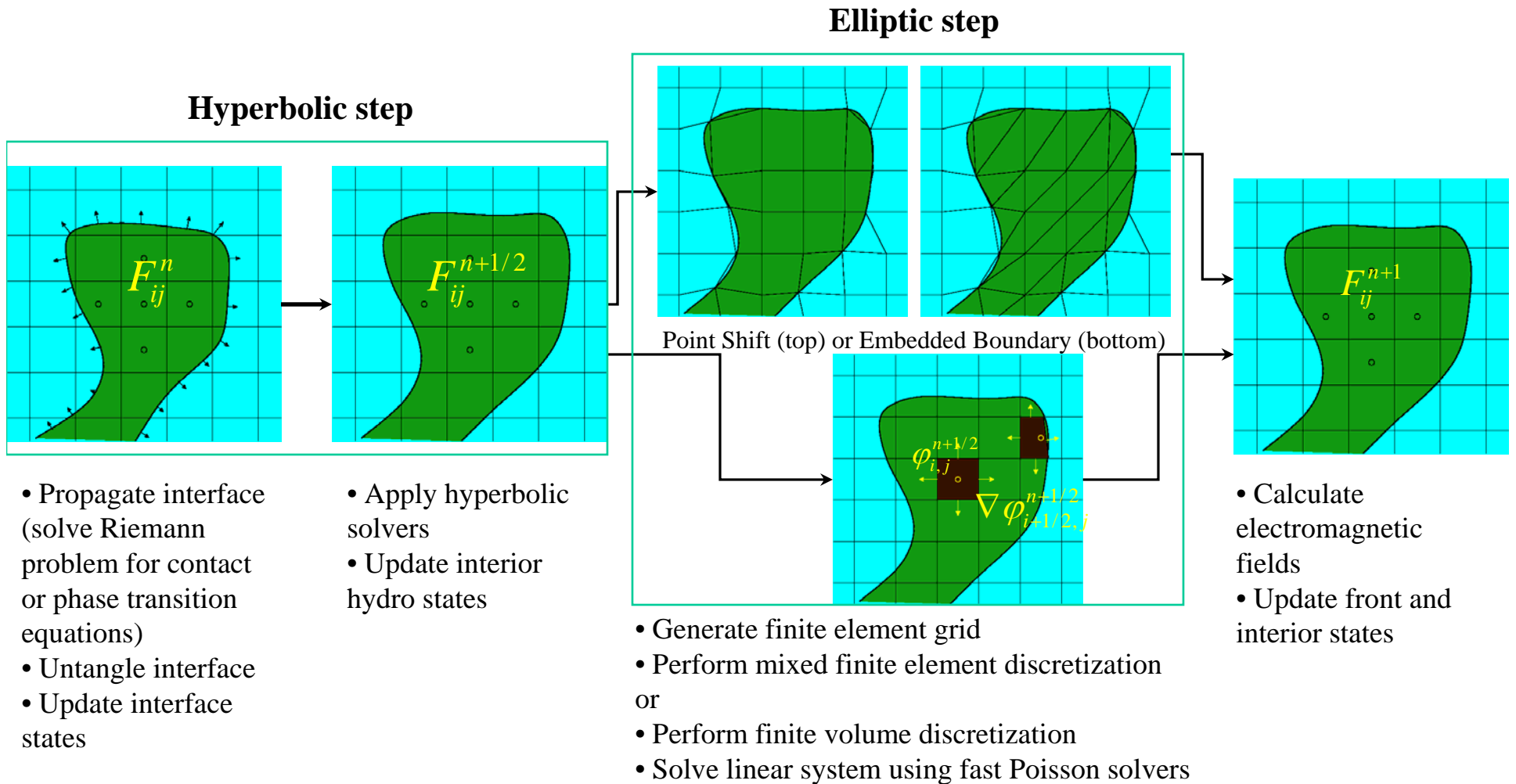
$$\mathbf{J} = \sigma \left(-\nabla \phi + \frac{1}{c} \mathbf{u} \times \mathbf{B} \right)$$

$$\nabla \cdot \sigma \nabla \phi = \frac{1}{c} \nabla \cdot (\mathbf{u} \times \mathbf{B}),$$

$$\text{with } \left. \frac{\partial \phi}{\partial \mathbf{n}} \right|_{\Gamma} = \frac{1}{c} (\mathbf{u} \times \mathbf{B}) \cdot \mathbf{n}$$

$$\mathbf{B} = \mathbf{B}_{\text{ext}}(x, t), \quad \nabla \cdot \mathbf{B}_{\text{ext}} \equiv 0$$

FronTier-MHD numerical scheme



Normal propagation of interface points

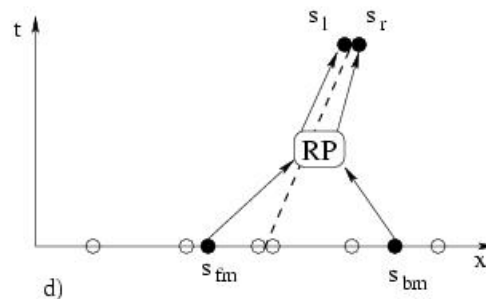
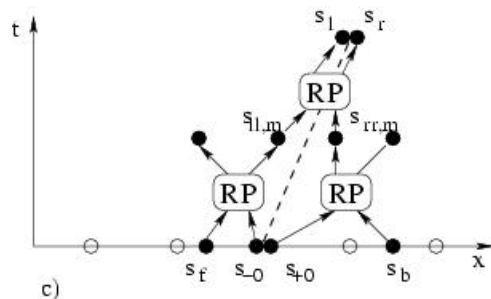
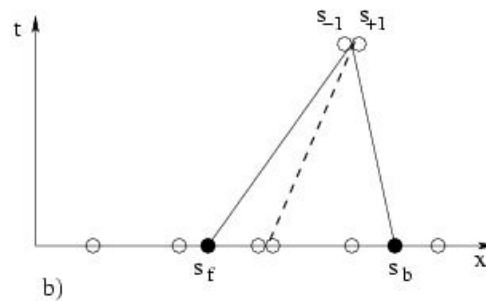
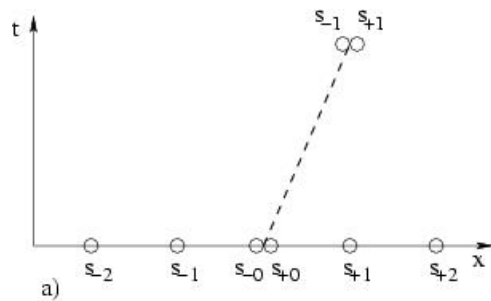
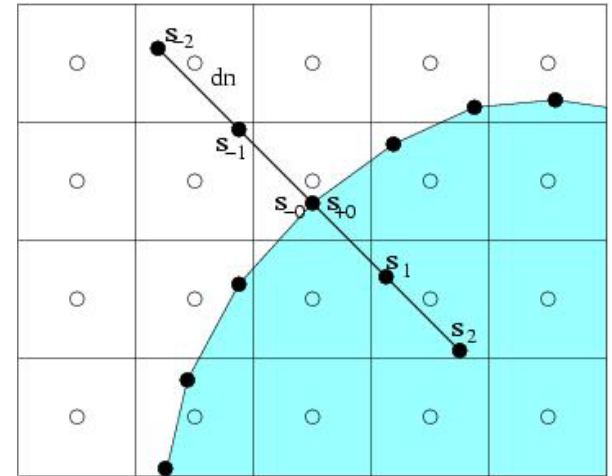
Contact discontinuity (no phase transition)

$$\frac{\partial \rho}{\partial t} + \frac{\partial \rho v_N}{\partial \mathbf{N}} + \frac{\alpha N_0}{r} \rho v_N = 0,$$

$$\frac{\partial \rho v_N}{\partial t} + \frac{\partial (\rho v_N^2 + P)}{\partial \mathbf{N}} + \frac{\alpha N_0}{r} \rho v_N^2 = \rho g_N + \frac{1}{c} (\mathbf{J} \times \mathbf{B})_N,$$

$$\frac{\partial \rho v_T}{\partial t} + \frac{\partial \rho v_N \mathbf{v}_T}{\partial \mathbf{N}} + \frac{\alpha N_0}{r} \rho v_N \mathbf{v}_T = 0,$$

$$\frac{\partial \rho E}{\partial t} + \frac{\partial (\rho E v_N + P v_N)}{\partial \mathbf{N}} + \frac{\alpha N_0}{r} (\rho E v_N + P v_N) = \rho g_N v_N$$



Phase boundary problem

Interface jump conditions

$$[\rho u] = s[u]$$

$$[\rho u^2 + P] = s[\rho u]$$

$$[\rho u E + uP - \kappa \nabla T] = s[\rho E]$$

Balance equations

$$M = \frac{u_v - u_l}{\tau_v - \tau_l}, \quad \tau = \frac{1}{\rho},$$

$$M^2 = \frac{P_v - P_l}{\tau_v - \tau_l}, \quad (u_v - s)(u_l - s) = \frac{P_v - P_l}{\rho_v - \rho_l},$$

$$e_l - e_v + \frac{P_v - P_l}{2} (\tau_l - \tau_v) = \frac{1}{M} (\kappa_v T_{v,x} - \kappa_l T_{l,x})$$

Temperature and pressure at the interface

$$T_l = T_v = T_s$$

$$M = \alpha \frac{P_{sat}(T_s) - P_v}{\sqrt{2\pi RT_s}}, \quad P_{sat} = P_0 \exp\left(\frac{QM_{mol}}{R} \left(\frac{1}{T_0} - \frac{1}{T_s}\right)\right)$$

Most close work: Y. Matsumoto, F. Takemura, JSME Int. J., 37, 288-296, 1994.

Phase transition algorithm

- Standard contact discontinuity propagation: prediction step (Riemann problem) and the correction step (method of characteristics)
- There is no prediction step in the phase boundary problem: the solution structure is not known.
 - Method of characteristics step moves boundary points and updates boundary states
- The phase boundary algorithms consist of a hydro iteration and thermal iteration
 - In the hydro iteration, characteristics equations are solved to find the pressure and velocity

$$\frac{dp}{d\lambda_0} \pm \rho c \frac{du}{d\lambda_0} = \Gamma \kappa T_{xx}, \quad \frac{de}{d\lambda_{\pm}} + \rho \frac{dT}{d\lambda_{\pm}} = \frac{1}{\rho} \kappa T_{xx}$$

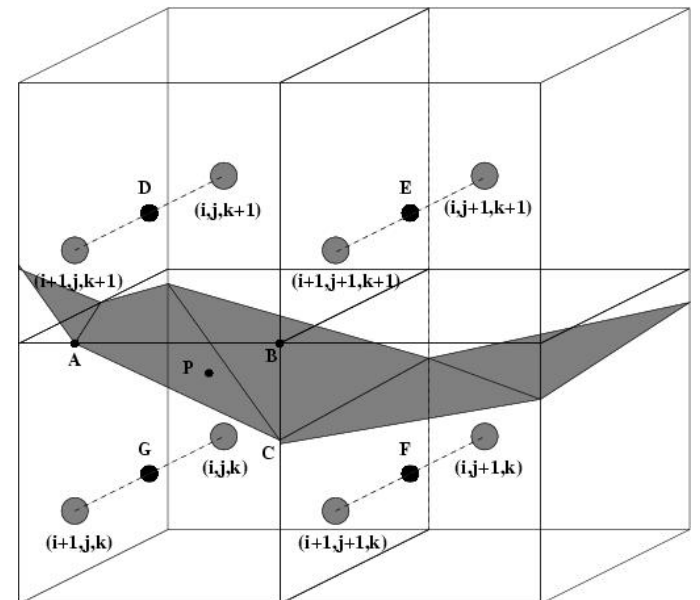
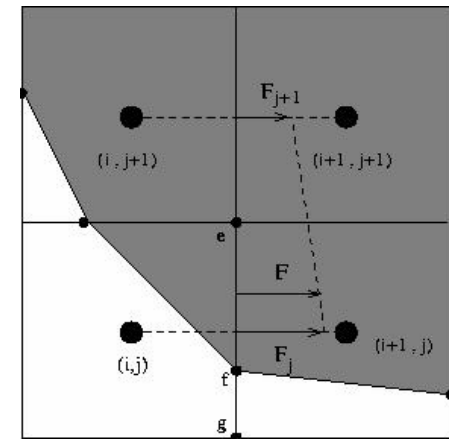
- In the thermal iteration, interface temperature and mass flux are found
 - Thin thermal layer near the interface. Subgrid model for temperature:

$$T \approx T_s + (T_{-1} + T_s) \operatorname{erf} \left(\frac{x}{\sqrt{4t\kappa/\rho c_p}} \right)$$

Embedded Boundary Elliptic Solver

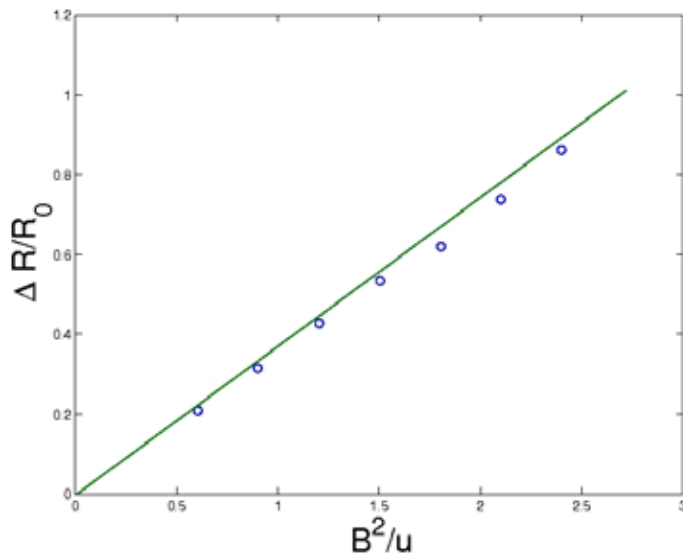
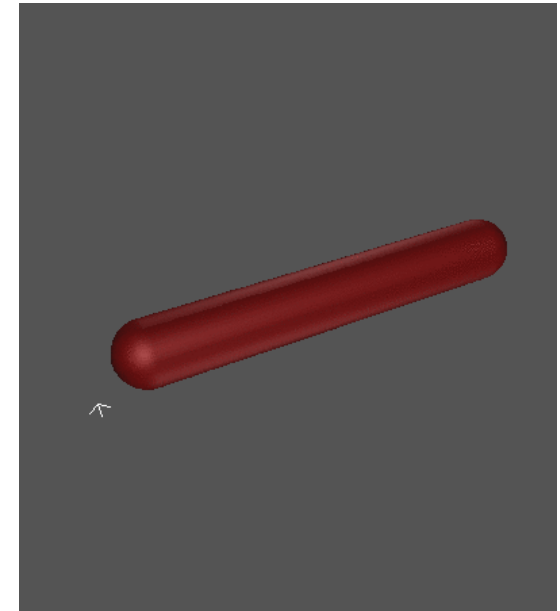
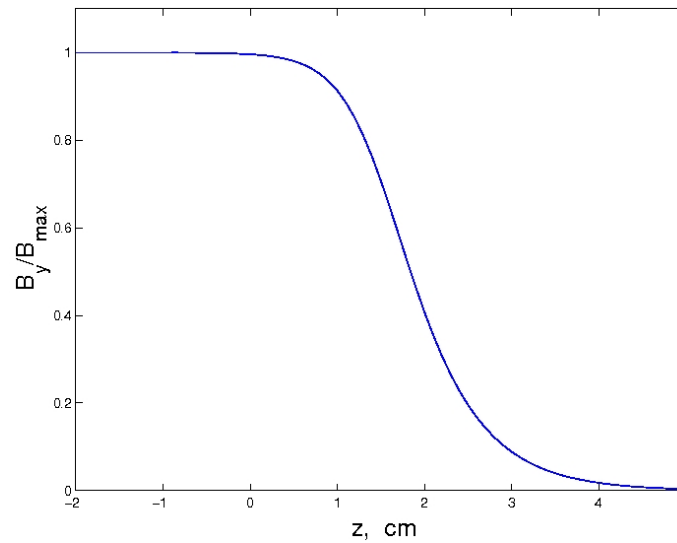
Main Ideas

- Based on the finite volume discretization
- Domain boundary is embedded in the rectangular Cartesian grid, and the solution is treated as a cell-centered quantity
- The discretized operator is centered in centroids of partial cells
- Using finite difference for full cell and linear interpolation for cut cell flux calculation

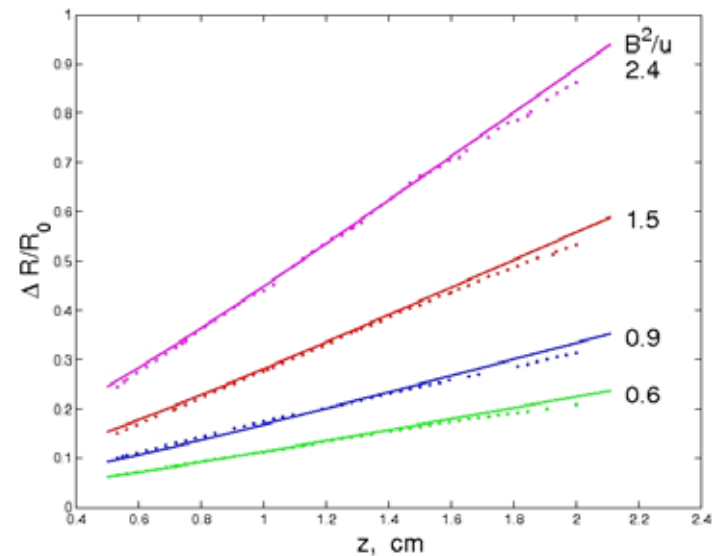


MHD code validation: entrance of a mercury jet in a transverse magnetic field

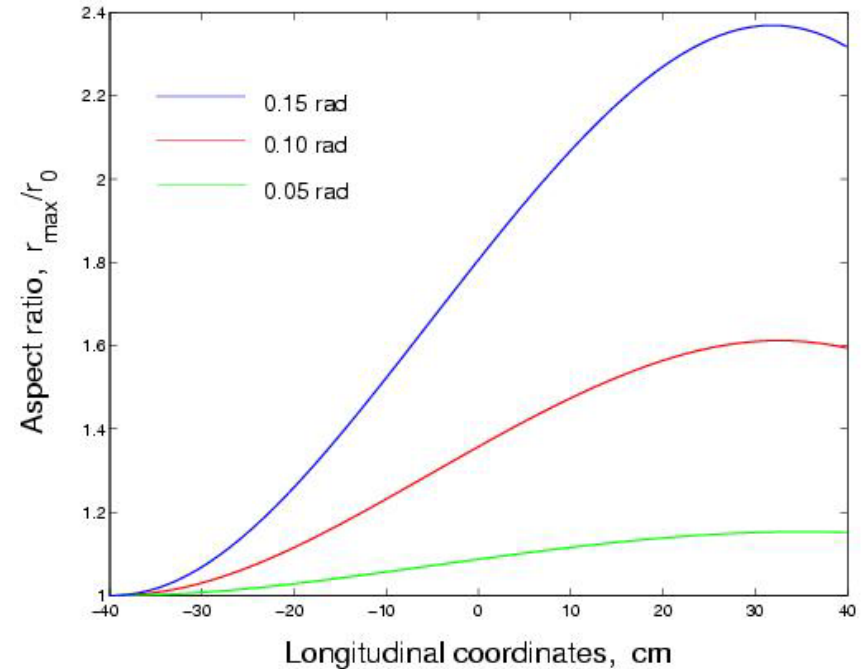
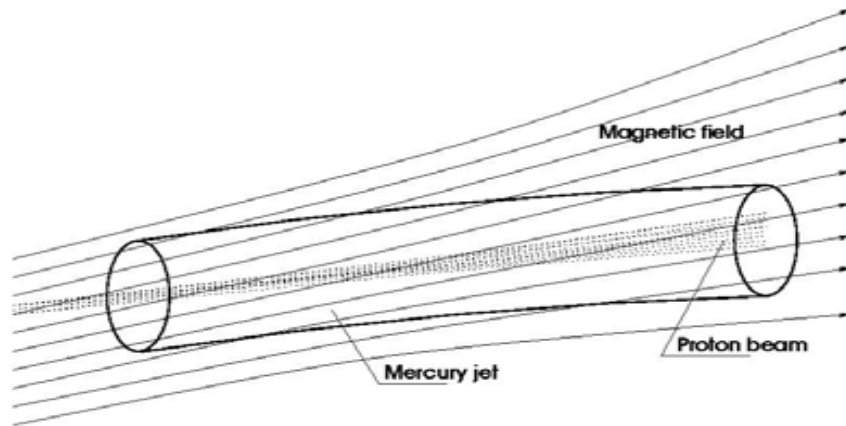
B-field profile



Comparison to analytical solutions (expansion series)



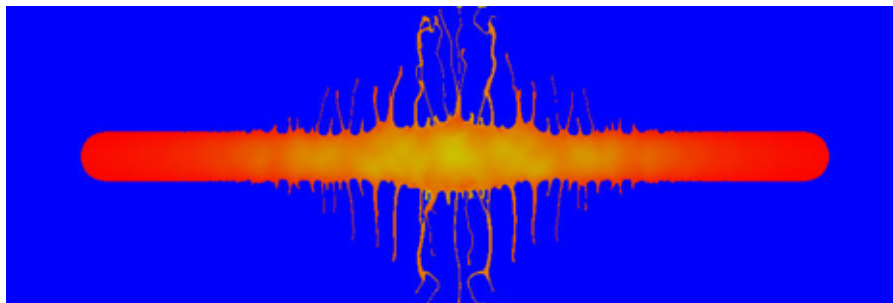
Muon Collider target: jet entrance in magnetic field



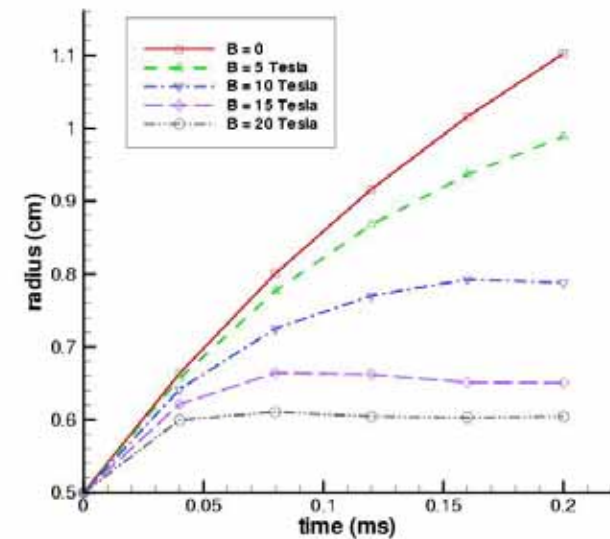
- Under the original design (0.1 rad entrance) the jet would transform into a fluid sheet
 - Greatly reduced cross-section with the proton pulse -> low particle production rate
- Our studies led to the change of design parameters of the future CERN experiment called MERIT

Muon Collider target: jet - proton pulse interaction

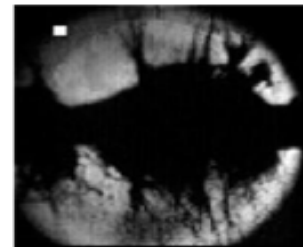
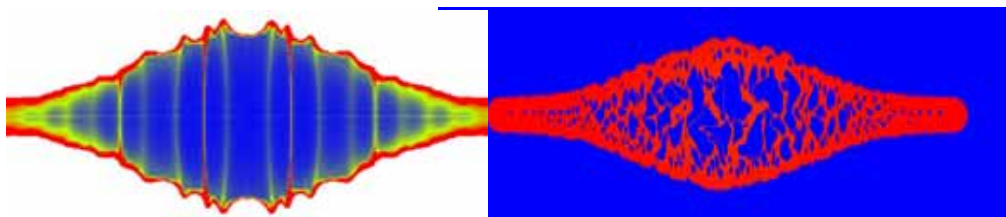
- Simulation of the mercury jet target interacting with a proton pulse in a magnetic field
 - Studies of surface instabilities, jet breakup, and cavitation
 - MHD forces reduce both jet expansion, instabilities, and cavitation



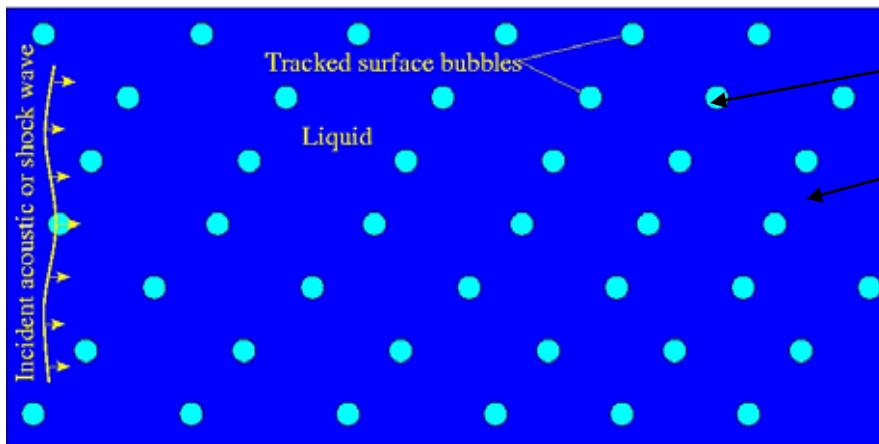
Jet surface instabilities



Cavitation in the mercury jet and thimble



Validation of Front Tracking method for small void fraction flows (bubbly and cavitating fluids)

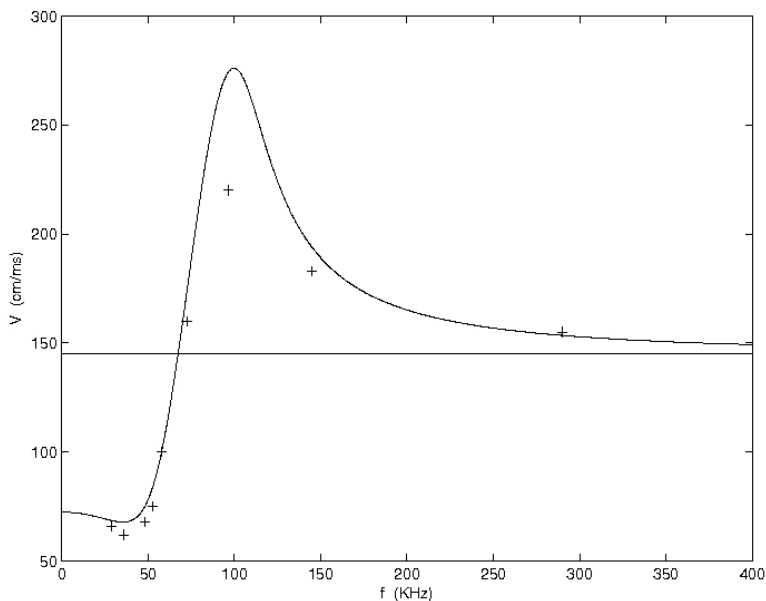


Polytropic EOS for gas (vapor) bubbles

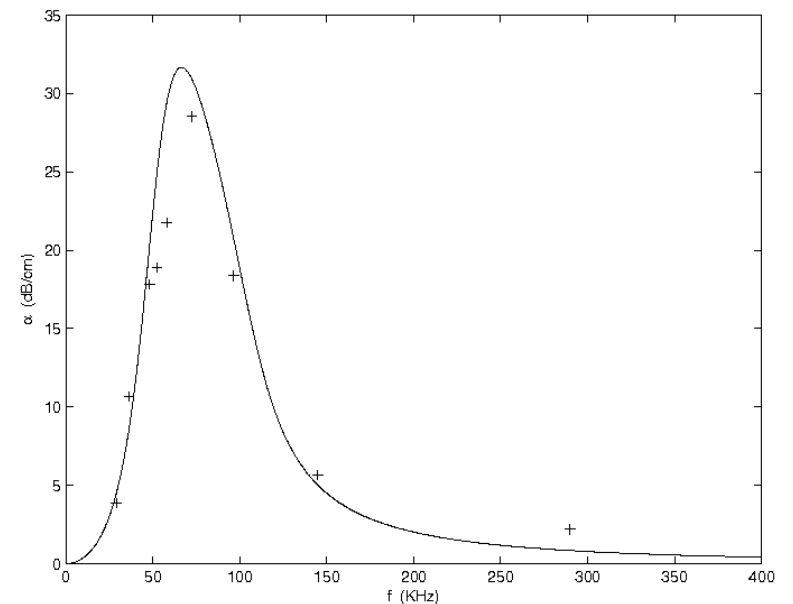
Stiffened Polytropic EOS for liquid

DNS of sound waves in bubbly liquids at extremely small void fractions: 0.02 %

Dispersion of sound waves

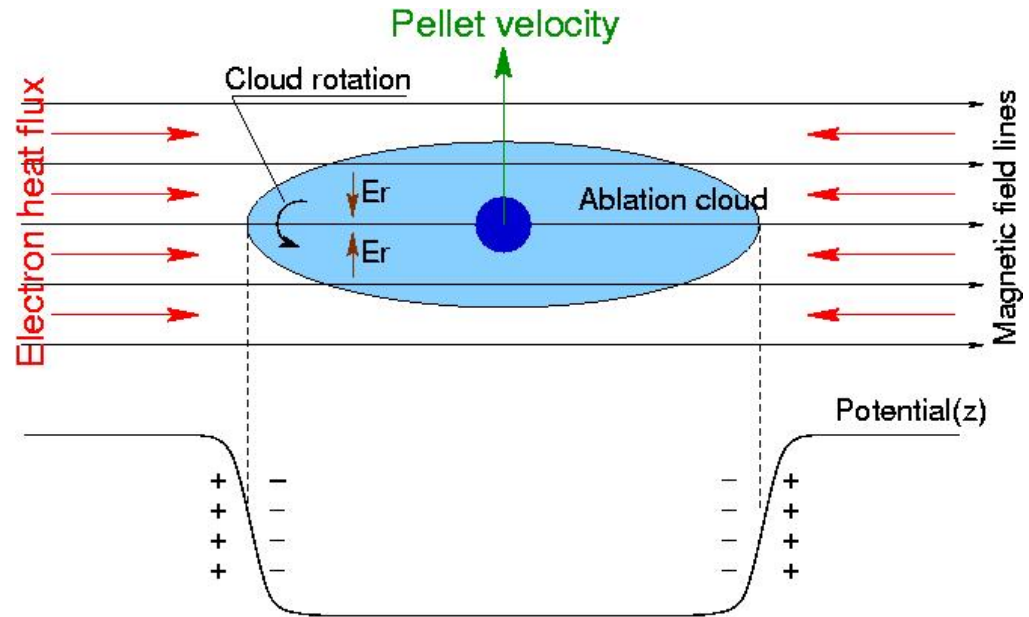


Attenuation of sound waves



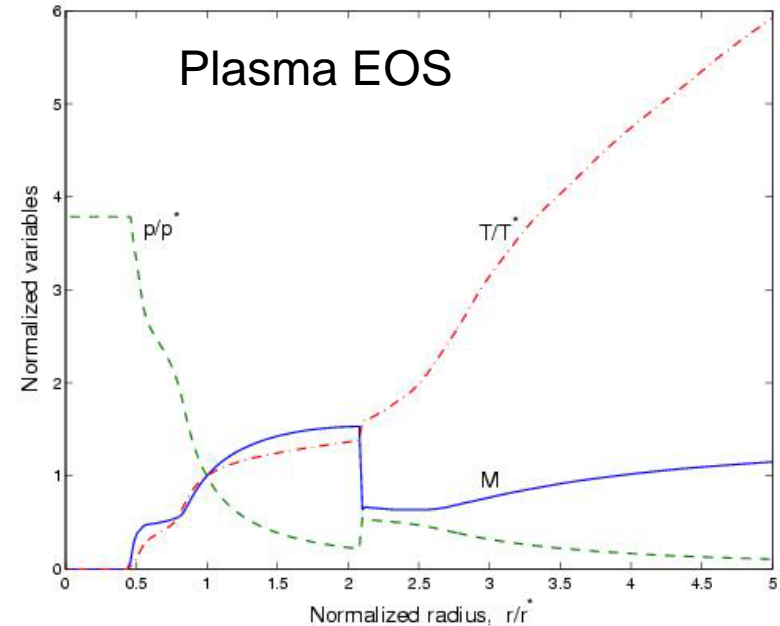
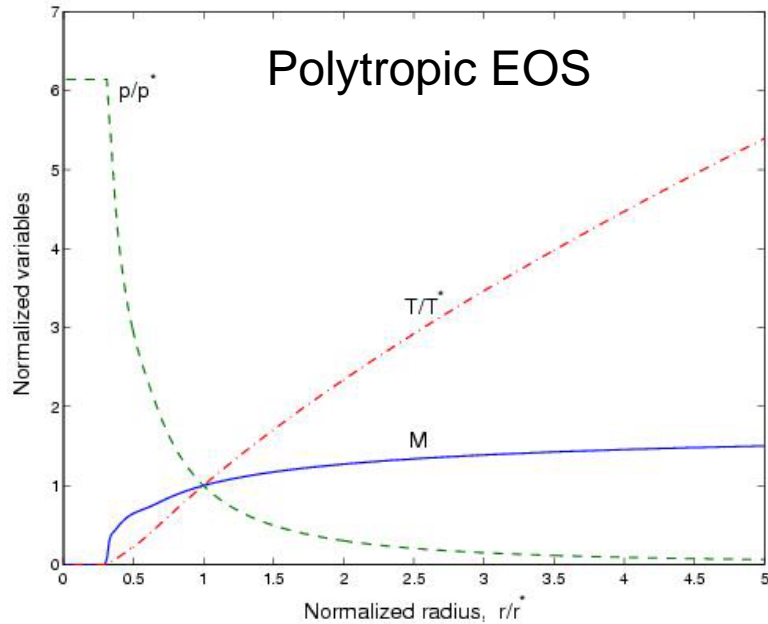
Pellet Ablation for Tokamak Fueling: Main Models

Schematic of processes in the ablation cloud



- Kinetic model for the interaction of hot electrons with the ablated gas
- Surface ablation model
- Equation of state with atomic processes
- Cloud charging and rotation models
- New conductivity model (ionization by electron impact)

Spherically symmetric problem - benchmark of the pellet ablation model



Normalized ablation gas profiles at 10 microseconds

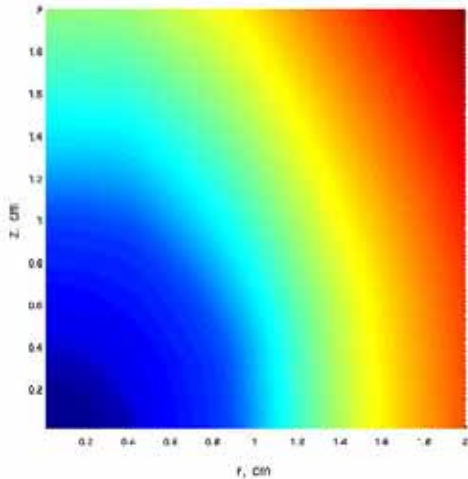
	Poly EOS	Plasma EOS
Sonic radius	0.66 cm	0.45 cm
Temperature	5.51 eV	1.07 eV
Pressure	20.0 bar	26.9 bar
Ablation rate	112 g/s	106 g/s

- Excellent agreement with TF model and Ishizaki.
- Verified scaling laws of the TF model

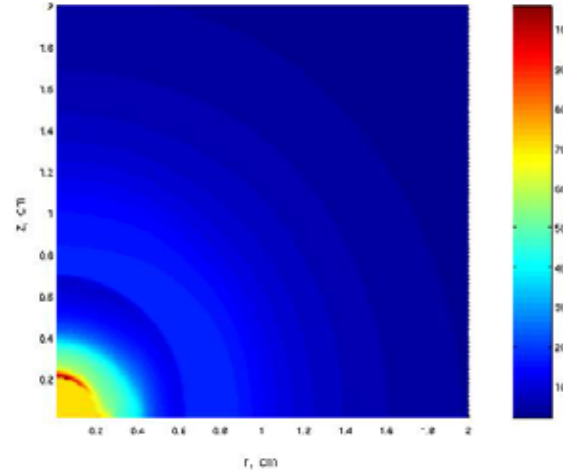
$$G \sim r_p^{4/3}$$

$$M_\infty = \sqrt{\frac{5}{\gamma}} = 1.8898 \quad \left(\text{for } \gamma = \frac{7}{5} \right)$$

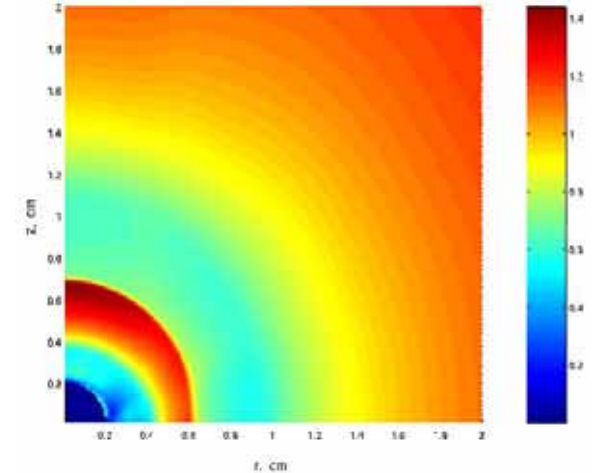
Axially Symmetric Hydrodynamic Problem



Temperature, eV



Pressure, bar

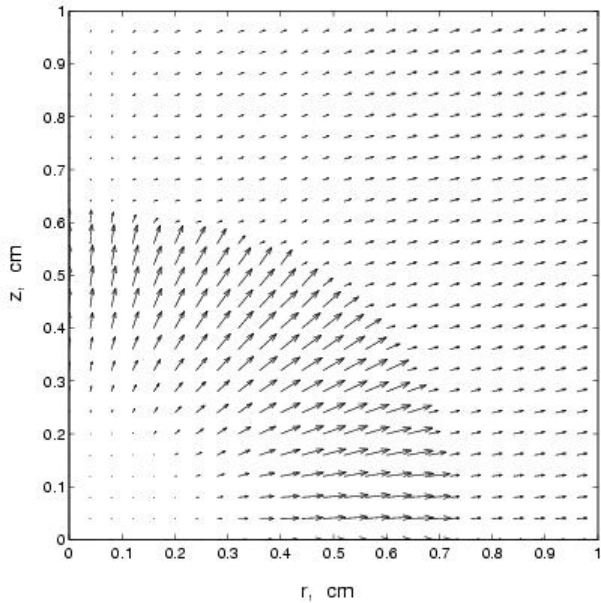


Mach number

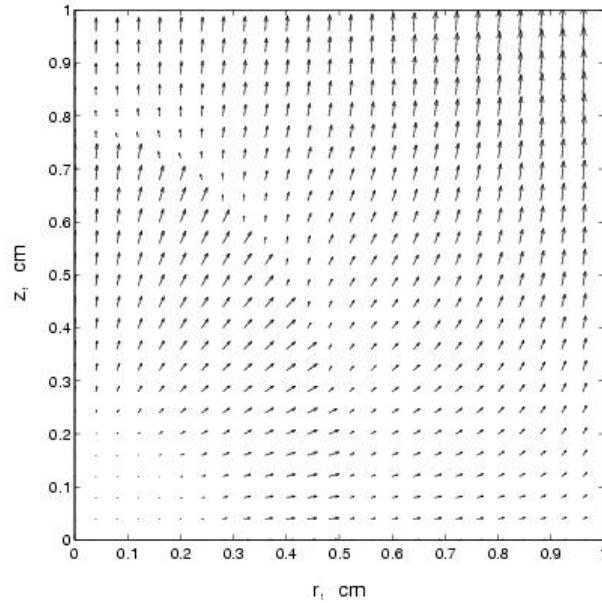
Distributions of temperature, pressure, and Mach number of the ablation flow near the pellet at 20 microseconds.

- We explained the **factor of 2.2 reduction** of the ablation rate
 - In the literature, it was **incorrectly** attributed to the directional heating
 - We showed that the directional heating reduces the ablation rate by 18%
 - The 2.2 factor was caused by Maxwellian electron heat flux vs. monoenergetic

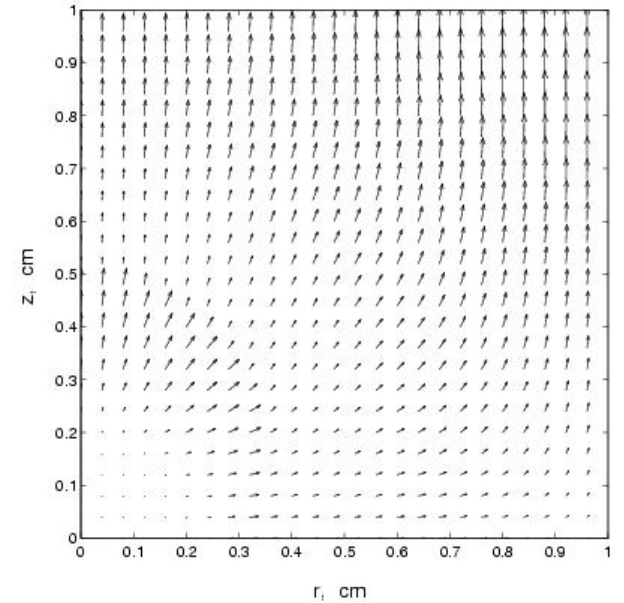
Axially symmetric MHD simulation (2.5D model) (First MHD simulation of detailed pellet ablation physics)



1 microsecond



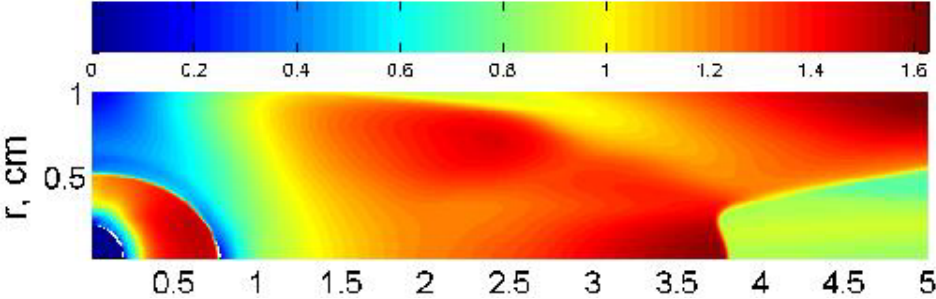
2 microseconds



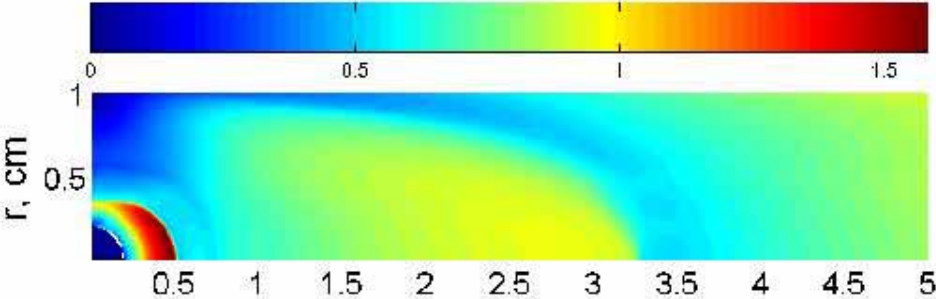
3 microseconds

Velocity distribution of the ablation flow near the pellet in 6 Tesla magnetic field. Warm up time is 20 microseconds.

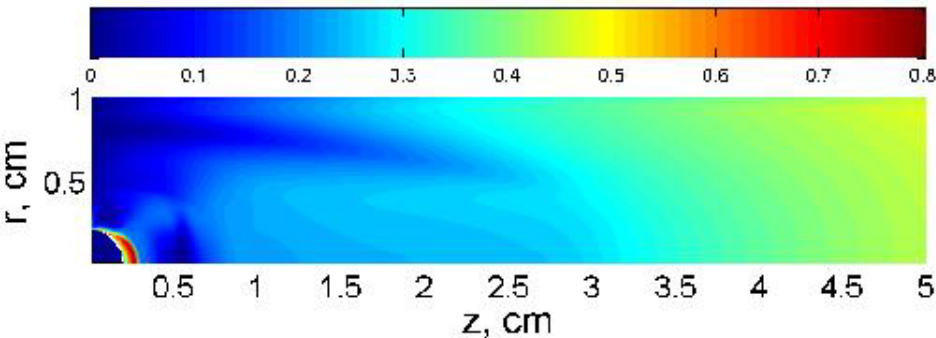
Mach number distribution of the ablation flow near the pellet in 6 Tesla magnetic field. Warm up time is 20 microseconds.



3 microseconds

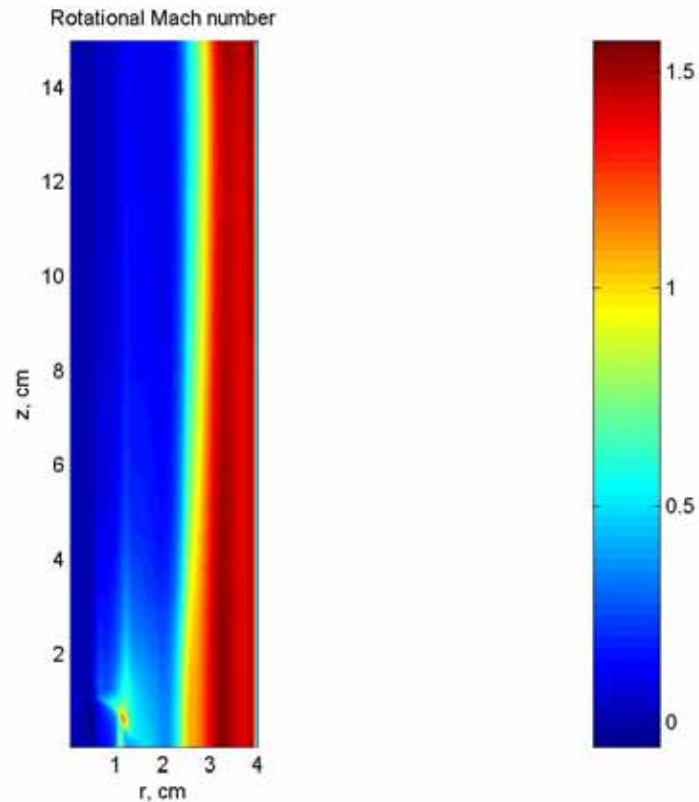


5 microseconds



9 microseconds

Rotation of the ablation channel (2.5D model)

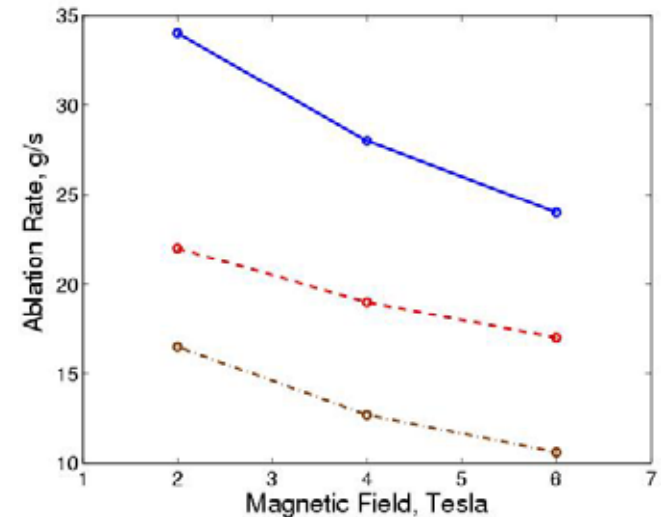


- Supersonic rotation of the channel layers due to the $E \times B$ force
- Density re-distribution (pipe-like)

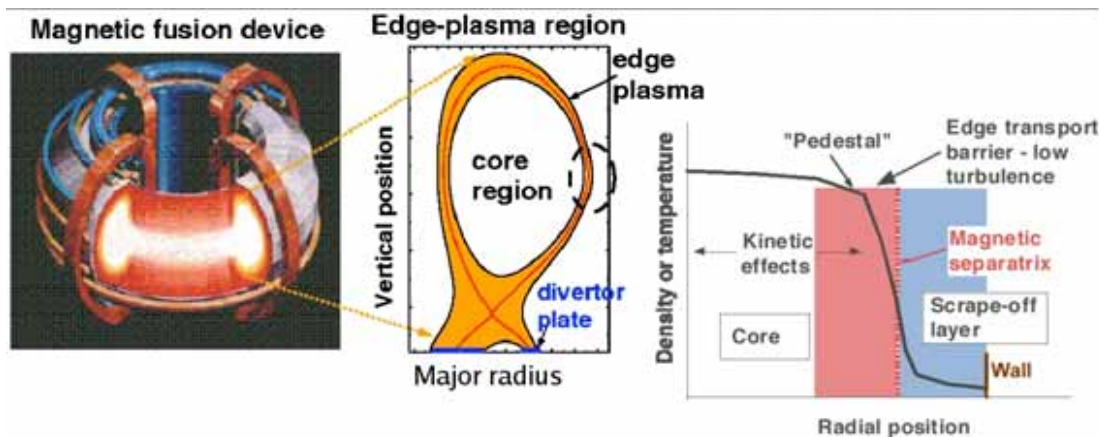
Formation of the ablation channel in the pedestal

Critical observation:

- **Formation of the ablation channel strongly depends on the pedestal properties**
- Channel radius depends on the warm-up time (pedestal width/pellet velocity)
- Ablation rate strongly depends on the channel radius
- In ITER, fast pellets in narrow pedestal region will result in narrow channels and small ablation rate



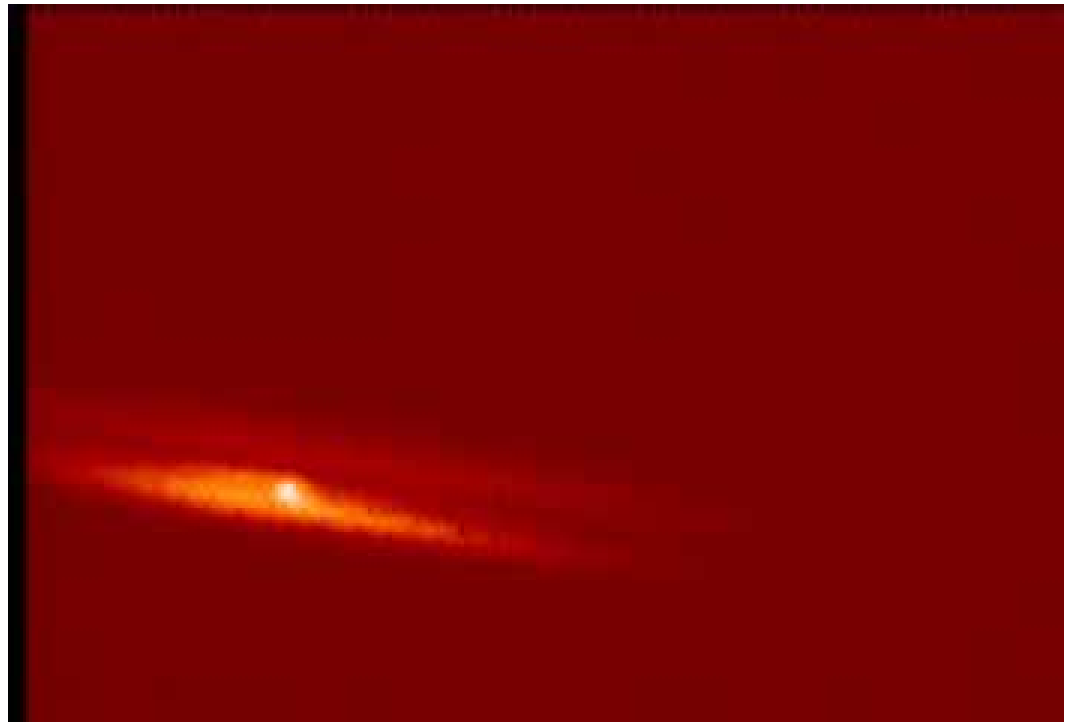
Solid line: $t_w = 10, n_e = 1.0e14 \text{ cm}^{-3}$
 Dashed line: $t_w = 10, n_e = 1.6e13 \text{ cm}^{-3}$
 Dotted line: $t_w = 5, n_e = 10e14 \text{ cm}^{-3}$ □



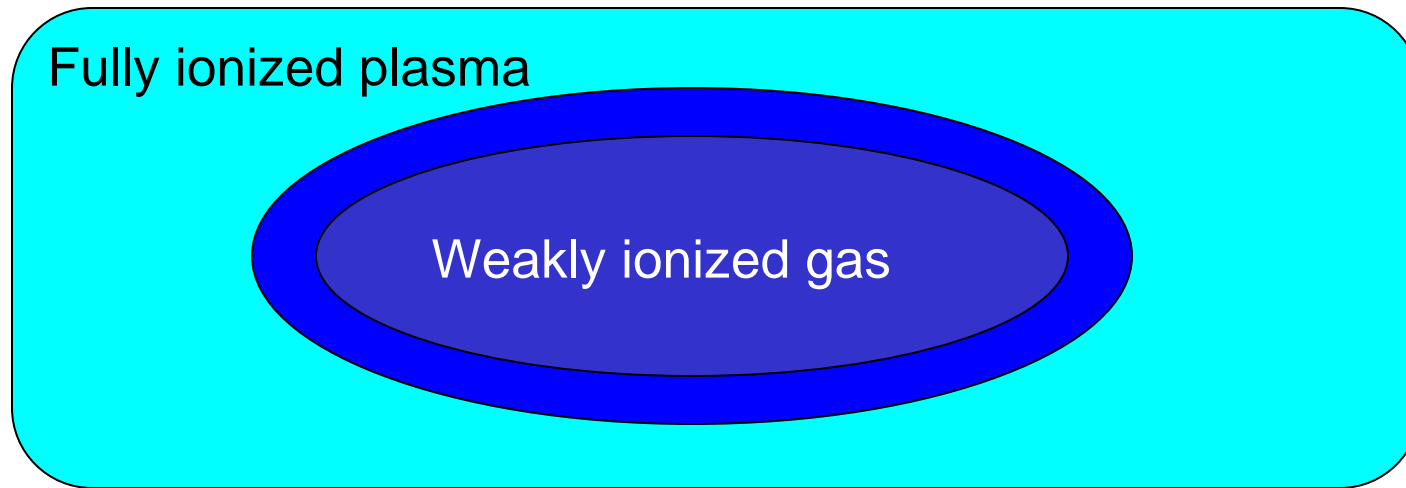
Current work: 3D pellet ablation simulation

- Full 3D model employs physics models similar to 2.5D model
 - More complex algorithms for the potential distribution
- Expected to shed light on the nature of striation instabilities

**Striation instabilities:
Experimental observation
(Courtesy MIT Fusion Group)**



Future Plans: Adding Fully Ionized Plasma Domain

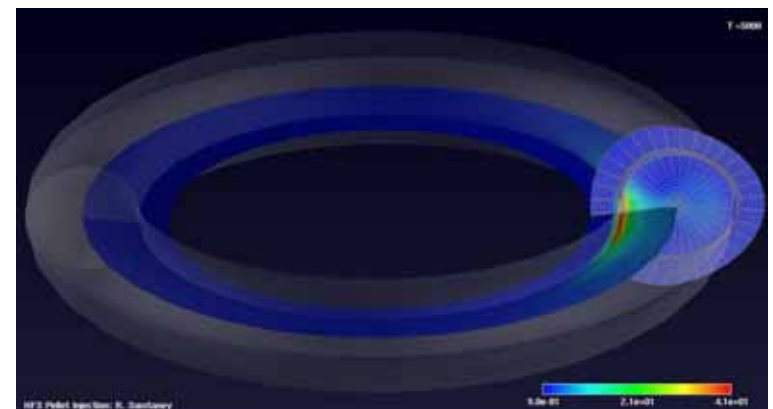


In overlapping region, both solutions are assumed to be approximately valid; weighted sum of two solutions

- Coupling of FronTier-MHD as a subgrid model with PPPL plasma code
 - Heterogeneous multiscale coupling
 - Address mathematical/numerical issues of the coupling (numerical stability and error)

Previous Studies: Global Models (examples)

- Simulations using MH3D code, H. Strauss & W. Park, 1998
 - Finite element version of the MH3D full MHD code
 - Details of the ablation are not considered
 - Pellet is given as a density perturbation of initial conditions
 - Smaller values of density and larger pellet radius (numerical constraints)
- Simulations using MHD code based on CHOMBO AMR package, R. Samtaney, S. Jardin, P. Colella, D. Martin, 2004
 - Analytical model for the pellet ablation: moving density source
 - 8-wave upwinding unsplit method for MHD
 - AMR package – significant improvement of numerical resolution



Future Needs of the ITER Fueling Simulation

- Coupling is required by the next level of ITER fueling simulations
- Neither plasma MHD code nor FronTier are capable of performing refined ITER fueling simulation alone:
 - Plasma MHD code is not accurate in calculating thermodynamic states in the ablation channel and not capable of calculating the ablation rate
 - FronTier is not suitable for the entire tokamak study
 - FronTier ablation model uses several model parameters which are presently not calculated self-consistently
- A coupled simulation will resolve all current problems:
 - Self consistent calculation of all current model parameters
 - Resolution of detailed physics of the ablation channel in real tokamak
 - Simulation of the ablation channel evolution
 - Pellet ablation induced plasma instabilities

Conclusions

- Developed and validated a front tracking based algorithm for free surface MHD flows in the low magnetic Re approximation
- Developed phase transition algorithm for compressible fluids
- Validated front tracking based DNS of bubbly fluids at small void fractions
- Developed numerical models specific to the pellet ablation problem
 - Kinetic models for the electron heat deposition and hot currents
 - Equation of state in the presence of atomic processes
 - Surface ablation model
 - Model for the cloud potential
- Performed simulations of accelerator targets and pellet ablation in tokamaks